

X-RAY PROBES OF COSMIC STAR-FORMATION HISTORY

Pranab Ghosh^{1,2} & Nicholas E. White²

¹Tata Institute of Fundamental Research, Bombay 400 005, India

²NASA Goddard Space Flight Center, Greenbelt, MD 20771

Received _____; accepted _____

ABSTRACT

We discuss the imprints left by a cosmological evolution of the star formation rate (SFR) on the evolution of X-ray luminosities L_X of normal galaxies, using the scheme proposed by White and Ghosh (1998, WG98), wherein the evolution of L_X of a galaxy is driven by the evolution of its X-ray binary population. As indicated in WG98, the profile of L_X with redshift can both serve as a diagnostic probe of the SFR profile and constrain evolutionary models for X-ray binaries. We report here the first calculation of the expected evolution of X-ray luminosities of galaxies, updating the WG98 work by using a suite of more recently developed SFR profiles that span the currently plausible range. The first *Chandra* deep imaging results on L_X -evolution are beginning to probe the SFR profile of bright spirals: the early results are consistent with predictions based on current SFR models. Using these new SFR profiles, the resolution of the “birthrate problem” of low-mass X-ray binaries (LMXBs) and recycled, millisecond pulsars (WG98) in terms of an evolving global SFR is more complete. We discuss the possible impact of the variations in the SFR profile of individual galaxies and galaxy-types.

Subject headings: binaries: close—stars: formation—stars: evolution— galaxies: evolution—X-rays: galaxies—X-rays: stars

1. INTRODUCTION

The global star-formation rate (SFR) has undergone strong cosmological evolution: it was ~ 10 times its present value at $z \approx 1$, had a peak value ~ 10 – 100 times the present one in the redshift range $z \sim 1.5$ – 3.5 , and declined again at high z (Madau *et al.* 1996; Madau, Pozzetti & Dickinson 1998, M98; Blain, Smail, Ivison & Kneib 1999, B99a; Blain *et al.* 1999,

B99b, and references therein). Details of the SFR at high redshifts are still somewhat uncertain, because much of the star formation at $2 \lesssim z \lesssim 5$ may be dust-obscured and so missed by optical surveys, but detected readily through the copious submillimeter emission from the dust heated by star formation (Hughes *et al.* 1998; Barger *et al.* 1999).

The X-ray emission of a normal galaxy (*i.e.*, one without an active nucleus) is dominated by the integrated emission of the galaxy’s X-ray binary population (see, *e.g.*, Fabbiano 1995). In WG98 we discussed the effects of an evolving SFR on the evolution of X-ray binary populations of galaxies, and so on that of the X-ray emission from normal galaxies. We suggested that X-ray luminosities L_X of normal galaxies could show significant evolution (by up to a factor ~ 10), even in the relatively nearby redshift range $z \sim 0.5$ –1.0. We also showed that an evolving SFR could resolve the “birthrate problem” involving LMXB and their descendant “millisecond” radio pulsars (MRP, see Kulkarni & Narayan 1988; Lorimer 1995, L95).

The SFR profile used in WG98—the only profile available at the time—was based on the optical/UV data alone. Over the past three years, there has been considerable progress in our understanding of cosmic star-formation history. In addition, very deep X-ray imaging with *Chandra* is beginning to detect normal galaxies in the redshift range $z \sim 0.5$ –1.0, so that comparison with observations is becoming possible for the first time. In this *Letter*, we consider quantitatively the key imprints left by SFR evolution on the L_X -evolution profiles of normal galaxies, using the best SFR models currently available. We briefly discuss the recent results of Brandt *et al.* (2001, Bran01) from the ultradeep *Chandra* imaging of the Hubble Deep Field North (HDF-N). A detailed calculation of the expected X-ray flux distribution of the HDF-N galaxies based on the results of this paper is reported by Ptak *et al.* (2001, Ptak01). We also reconsider the resolution of the LMXB–MRP birthrate problem using the new SFR profiles, and find that the calculated

rates for both (a) whole populations of LMXB and MRP, and, (b) short-period systems, are consistent with observation for some SFR profiles suggested recently to account for the multiwaveband SFR data. We discuss the relative roles of global SFR profiles on the one hand, and the profiles of individual galaxies or galaxy-types on the other.

2. X-RAY LUMINOSITY EVOLUTION WITH EVOLVING SFR

The total X-ray output of a normal galaxy can be modeled as the sum of those of its HMXB and LMXB as per the WG98 scheme, wherein the evolution of each species “ i ” is described by a timescale τ_i (see WG98). To study the effects of the dependence of τ_i on the binary period and other evolutionary parameters, we run the evolutionary scheme over ranges of likely values of τ_i given in the literature. The evolution of the HMXB population in response to an evolving star-formation rate $\text{SFR}(t)$ is given by

$$\frac{\partial n_{\text{HMXB}}(t)}{\partial t} = \alpha_h \text{SFR}(t) - \frac{n_{\text{HMXB}}(t)}{\tau_{\text{HMXB}}}, \quad (1)$$

where n_{HMXB} is the number density of HMXBs in the galaxy, and τ_{HMXB} is the HMXB evolution timescale. α_h is the rate of formation of HMXBs per unit SFR, given approximately by $\alpha_h = \frac{1}{2} f_{\text{binary}} f_{\text{prim}}^h f_{\text{SN}}^h$, where f_{binary} is the fraction of all stars in binaries, f_{prim}^h is that fraction of primordial binaries which has the correct range of stellar masses and orbital periods for producing HMXBs (van den Heuvel 1992, vdH92 and the references therein), and $f_{\text{SN}}^h \approx 1$ is that fraction of massive binaries which survives the first supernova. In these calculations, we have adopted a representative value $\tau_{\text{HMXB}} \sim 5 \times 10^6$ yr according to current evolutionary models. In our introductory model here, τ_{HMXB} includes both (a) the time taken ($\sim 4 - 6 \times 10^6$ yr) by the massive companion of the neutron star to evolve from the instant of the neutron-star-producing supernova to the instant when the “standard” HMXB phase begins, and, (b) the duration ($\sim 2.5 \times 10^4$ yr) of this HMXB phase (vdH92 and references therein). Since the second timescale is negligible compared to

the first, little error is made by approximating this two-step process by a single step with an overall timescale τ_{LMXB} .

Two basic methods of LMXB production have been discussed. In the cores of dense globular clusters, they can be produced by the tidal capture of a neutron star by a normal star. Over the rest of a galaxy, stellar densities are insufficient for tidal capture, and LMXBs are produced by the evolution of primordial binaries (see, *e.g.*, Webbink, Rappaport & Savonije 1983; Webbink 1992). In this paper, we consider only the latter mechanism. For spiral galaxies, at least, this must be the dominant mechanism, since the globular-cluster LMXB population in such galaxies only accounts for a relatively small fraction of the total X-ray luminosity.

LMXB evolution from primordial binaries has two distinct stages (WG98) after the supernova produces a post-supernova binary (PSNB) containing the neutron star. First, the PSNB evolves on a timescale τ_{PSNB} due to nuclear evolution of the neutron star’s low-mass companion and/or decay of binary orbit due to gravitational radiation and magnetic braking, until the companion comes into Roche lobe contact and the LMXB turns on. Subsequently, the LMXB evolves on a timescale τ_{LMXB} . Since τ_{PSNB} and τ_{LMXB} are comparable in general, we must describe the two stages separately (WG98) by:

$$\frac{\partial n_{\text{PSNB}}(t)}{\partial t} = \alpha_l \text{SFR}(t) - \frac{n_{\text{PSNB}}(t)}{\tau_{\text{PSNB}}}, \quad (2)$$

$$\frac{\partial n_{\text{LMXB}}(t)}{\partial t} = \frac{n_{\text{PSNB}}(t)}{\tau_{\text{PSNB}}} - \frac{n_{\text{LMXB}}(t)}{\tau_{\text{LMXB}}}, \quad (3)$$

Here, n_{PSNB} and n_{LMXB} are the respective number densities of PSNB and LMXB in the galaxy, and α_l is the rate of formation of LMXB per unit SFR, given approximately by $\alpha_l = \frac{1}{2} f_{\text{binary}} f_{\text{prim}}^l f_{\text{SN}}^l$, where f_{binary} is the fraction of all stars in binaries, f_{prim}^l is that fraction of primordial binaries which has the correct range of stellar masses and orbital periods for producing LMXBs, and f_{SN}^l is that fraction of such binaries which survives the massive star’s supernova.

We display evolution in terms of the redshift z , which is related to the cosmic time t by $t_9 = 13(z + 1)^{-3/2}$, where t_9 is t in units of 10^9 yr, and a value of $H_0 = 50 \text{ km s}^{-1} \text{ Mpc}^{-1}$ has been used¹. We consider the suite of current SFR models detailed in Table 1 to cover a plausible range, using the parameterization of B99a,b. Models of the “peak” class have the form

$$\text{SFR}_{\text{peak}}(z) = 2 \left(1 + \exp \frac{z}{z_{\text{max}}} \right)^{-1} (1 + z)^{p + \frac{1}{2z_{\text{max}}}}, \quad (4)$$

while those of the “anvil” class have the form

$$\text{SFR}_{\text{anvil}}(z) = \begin{cases} (1 + z)^p, & z \leq z_{\text{max}}, \\ (1 + z_{\text{max}})^p, & z > z_{\text{max}}. \end{cases} \quad (5)$$

These functional forms are not unique, but useful, since they have a convenient low- z limit, $\text{SFR}(z) \propto (1 + z)^p$, where all SFR profiles must agree with the optical/UV data (M98), and since the model parameters can be manipulated to mimic a wide range of star-formation histories (B99b). Peak-class profiles are useful for describing (a) SFRs determined from optical/UV observations, *i.e.*, Madau-type (M98) profiles, called “Peak-M” in Table 1, and, (b) more general SFRs with enhanced star formation at high z , a good example of which is the “hierarchical” model of B99b, wherein the submillimeter emission is associated with galaxy mergers in an hierarchical clustering model of galaxy evolution. Anvil-class profiles are useful for describing the results of “monolithic” models. The “Gaussian” model (B99a,b) is an attempt at giving a good account of the SFR at both low and high z by making a composite of the Peak-G model (see Table 1) and a Gaussian starburst at a high

¹For ease of comparison with WG98 and M98, we continue to use here a Friedman cosmology with $q_0 = 1/2$; other cosmologies will be considered elsewhere. Other values of the Hubble constant lead to a straightforward scaling: for $H_0 = 70 \text{ km s}^{-1} \text{ Mpc}^{-1}$, for example, $t_9 \approx 10(z + 1)^{-3/2}$, so that the results remain unchanged if all timescales are shortened by a factor of 1.3.

redshift z_p , *i.e.*, a component

$$\text{SFR}_{\text{Gauss}}(z) = \Theta \exp \left\{ -\frac{[t(z) - t(z_p)]^2}{2\sigma^2} \right\}. \quad (6)$$

Based on the *IRAS* luminosity function, this component is devised to account for the high- z data, particularly the submillimeter observations (B99a). For its parameters (see Table 1), we have used the revised values given in B99b. In all models considered here, no galaxies exist for sufficiently large redshifts, $z > 10$.

Figures 1 and 2 show the prompt evolution of HMXBs and the slow evolution of LMXBs, and the evolution of the total X-ray binary population, where the two components have been so weighted as to represent the total X-ray emission from the galaxy (the weight-ratio is the product of α_h/α_l and the ratio of the average luminosity of HMXBs and LMXBs). The HMXB profile closely follows the SFR profile because τ_{HMXB} is small compared to the SFR evolution timescale. By contrast, the LMXB profile has a significant lag behind the SFR profile because τ_{PSNB} and τ_{LMXB} are comparable to SFR evolution timescale: depending on these timescales, the LMXB profile peaks at redshifts ~ 1 – 3 later than the HMXB profile (as seen clearly in Figs. 1 and 2), which is a characteristic signature of SFR evolution (WG98).

Figure 1 compares the L_X -evolution corresponding to the (Madau or Peak-M) SFR profile and the evolutionary timescales we originally used in WG98, *i.e.*, (a) $\tau_{\text{PSNB}} = 1.9$ Gyr, $\tau_{\text{LMXB}} = 0.1$ Gyr for the whole LMXB population, and (b) $\tau_{\text{PSNB}} = 0.9$ Gyr, $\tau_{\text{LMXB}} = 0.5$ Gyr for the short-period systems. In Figure 2, we display the L_X -evolution for a range of SFR profiles—Peak-M, Hierarchical, Anvil-10, and Gaussian, the evolutionary timescales being held fixed at $\tau_{\text{PSNB}} = 1.9$ Gyr, $\tau_{\text{LMXB}} = 1.0$ Gyr. Between them, the two figures thus explore the effects of (a) varying the evolutionary timescales for a fixed SFR profile, *viz.* Peak-M, and (b) varying the profile for a fixed set of evolutionary timescales. For sufficiently *slow* LMXB evolution, the galaxy’s X-ray emission is dominated by LMXBs at

low redshifts ($0 \lesssim z \lesssim 1$), and by HMXBs at high redshifts. As a result, the total L_X -profile is *strongly* influenced at high redshifts by the SFR profile (see Fig.2), and may actually show hints of a double-peak structure (WG98) at intermediate redshifts (*e.g.*, the Gaussian profile in Fig.2). For sufficiently *fast* LMXB evolution, on the other hand, LMXBs and HMXBs may have comparable contributions to L_X at low redshifts (see Fig.1).

Bran01 estimate that the average X-ray luminosity of the bright spiral galaxies at an average redshift $z \approx 0.5$ used in their stacking analysis is about a factor of 3 higher than that in the local Universe ($z < 0.01$). This observed evolution, $L_X(0.5)/L_X(0.0) \sim 3$, can be compared with our theoretical results in Table 2. The degree of evolution from $z = 0$ to $z = 0.5$ – 1.0 increases from Madau-type profiles to those with additional star formation at high redshifts, the numbers for the Peak-M profile being in best agreement with Bran01. For a given profile, the evolutionary factor is smaller for a slower evolution of LMXBs (roughly measured in this context by the total time $\tau_{\text{PSNB}} + \tau_{\text{LMXB}}$), as expected. More sophisticated estimates of the expected L_X -distribution of HDF-N galaxies, based on these evolutionary scenarios, are described in Ptak01.

3. BIRTHRATE PROBLEM: FURTHER CONSIDERATIONS

As discussed in WG98, the evolution of MRPs from LMXBs is described by an equation similar to Eq. 3, but involving the MRP number density n_{MRP} , and MRP evolution timescale $\tau_{\text{MRP}} \sim 3 \times 10^9 - 3 \times 10^{10}$ yr (Camilo *et al.* 1994). Our evolutionary scheme yields the profiles of LMXB and MRP evolution for a given SFR profile, giving the number ratio, $N_r \equiv n_{\text{MRP}}/n_{\text{LMXB}}$, and the rate ratio, $R_r \equiv \frac{n_{\text{MRP}}}{\tau_{\text{MRP}}} / \frac{n_{\text{LMXB}}}{\tau_{\text{LMXB}}}$, of the MRP and LMXB populations at the present epoch ($z = 0$). We showed in WG98 that the Peak-M profile yielded $R_r \simeq 1$ for the overall MRP and LMXB populations, in agreement with current observations (L95). However, for short-period systems (LMXB periods $\lesssim 3$ days), this

profile yielded a value $R_r \simeq 3$, smaller than the current value $R_r \approx 8$ estimated from observations (L95). On repeating these calculations with other SFR profiles which have additional star formations at high redshifts, *e.g.*, the Gaussian and hierarchical profiles, we now find reasonable agreement for both whole populations and short-period systems, since these give $R_r \approx 6 - 8$ for short-period systems, for plausible evolutionary timescales. Thus, there appears to be no discrepancy between observation and the idea that SFR evolution naturally leads to values of R_r which can be ≈ 1 as well as considerably above unity (but see §4).

A new development in SFR research since WG98 has been the study of star-formation histories of individual galaxies and various galaxy-types. SFR profiles of individual galaxies, ranging from those in the Local Group to those in the HDF at redshifts $0.4 \lesssim z \lesssim 1$, have been inferred, using a variety of techniques (Glazebrook *et al.* 1999, Abraham *et al.* 2000, Hernandez *et al.* 2000). For various galaxy-types, models of Spectro-photometric evolution, which use the synthesis code *Pégase* and are constrained by deep galaxy counts, have been developed (Rocca-Volmerange and Fioc 2000), leading to a model SFR profile for each type. The birthrate problem was originally formulated entirely in terms of observations in our own galaxy, so that, strictly speaking, we should use the SFR profile of our galaxy. As none of the above techniques can be used in our own galaxy, it is difficult (but not impossible) to determine its SFR profile: calculations with such a profile will be described elsewhere.

4. DISCUSSION

We have shown that different global SFR profiles within the currently admissible range lead to very different L_X -evolution profiles, so that the latter profiles can be an *independent* X-ray probe of cosmic star-formation history. Our results and a more detailed consideration by Ptak01 indicate that the early *Chandra* results (Bran01) are consistent with the Peak-M

profile: let us now clarify the underpinnings of this result by applying the considerations of global and individual SFR profiles summarized above. Bran01 used bright spirals for their stacking analysis. Rocca-Volmerange and Fioc (2000) have shown that the model SFR profile for such (Sa-Sbc) spirals rises roughly in a Madau fashion from $z = 0$ to $z \approx 1$ (which these authors ascribe to a bias in the original sample used to construct the Madau profile towards bright spirals), and thereafter flattens to a roughly constant value ~ 12 times that at $z = 0$, falling again at $z \gtrsim 7$. We can roughly represent this profile in the range $0 < z \lesssim 7$ by an anvil-type profile (see §2), with the parameter z_{max} as given in Table 1, and the parameter $p \approx 2.7$. For such a profile with the timescales $\tau_{PSNB} = 1.9$ Gyr, $\tau_{LMXB} = 1.0$ Gyr, as in Figure 2, our evolutionary scheme gives $L_X(0.5)/L_X(0.0) = 3.3$, and $L_X(1.0)/L_X(0.0) = 5.4$, in good agreement with both the Bran01 results and the Peak-M results given in Table 2. We now see why the Peak-M profile appears to give a good account of the Bran01 results. In effect, the Bran01 analysis may be probing the SFR profile of only the bright spirals in HDF-N, and the fact that the Peak-M profile is consistent with the Bran01 results does *not* imply that the global SFR necessarily follows the Peak-M profile. Thus, there is no basic contradiction between the results of §2 and §3. However, the fact that our global analysis of the birthrate problem (§3) gives the best agreement with observation for SFR profiles (Gaussian and hierarchical) which have larger SFRs at high redshifts than the model Sa-Sbc profile of Rocca-Volmerange and Fioc (which, in turn, has a larger SFR at high redshifts than the Peak-M profile) remains to be understood fully. The individual-galaxy treatment may hold the key here.

Signatures of star formation in the relatively nearby ($z \lesssim 1$) Universe have usually been sought at wavelengths other than X-rays. In this redshift range, the X-ray probe described here is a “fossil record” study of star formation at earlier epochs for sufficiently slow LMXB evolution (see Fig.2), since LMXBs then preserve this record for ~ 1 Gyr after the star-formation peak is gone. Conversely, for a known SFR profile, this is a unique

proving ground for theories of LMXB evolution, which have been built almost wholly on the basis of our experience in the current epoch: this new probe is, at present, our only direct means of watching LMXB evolution unfold over cosmic time.

It is a pleasure to thank L. Angelini, R. Griffiths, R. Mushotzky, and A. Ptak for stimulating discussions.

REFERENCES

- Abraham, R. G., *et al.* 1999, MNRAS, 303, 641
- Barger, A. J., *et al.* 1998, Nature, 394, 248
- Blain, A. W., Smail, I., Ivison, R. J. & Kneib, J.-P. 1999, MNRAS, 302, 632 (B99a)
- Blain, A. W., Jameson, A., Smail, I., Longair, M. S., Kneib, J.-P. & Ivison, R. J. 1999, MNRAS, 309, 715 (B99b)
- Brandt, W. N. *et al.*, 2001, AJ, in press [astro-ph/0102411] (Bran01)
- Camilo, F., Thorsett, S.E. & Kulkarni, S.R. 1994, ApJ, 421, L15
- Fabbiano, G. 1995, in X-ray Binaries, ed. W. H. G. Lewin, J. van Paradijs and E. P. J. van den Heuvel, p.390
- Glazebrook, K., *et al.* 1999, MNRAS, 306, 843
- Hernandez, X., Gilmore, G. & Valls-Gabaud, D. 2000, MNRAS, 317, 831
- Hughes, D. H., *et al.* 1998, Nature, 394, 241
- Kulkarni, S. & Narayan, R. 1988 ApJ, 335, 755
- Lorimer, D. R. 1995, MNRAS, 274, 300 (L95)
- Madau, P., Ferguson, H. C., Dickinson, M. E., Giavalisco, M., Steidel, C. C., & Fruchter, A. 1996, MNRAS, 283, 1388
- Madau, P., Pozzetti, L., & Dickinson, M. 1998, ApJ, 498, 106 (M98)
- Ptak, A. *et al.*, ApJ, in press (Ptak01)

- Rocca-Volmerange, B. & Fioc, M. 2000, in Toward A New Millenium in Galaxy Morphology, ed. D. L. Block, I. Puerari, A. Stockton & D. Ferreira, Kluwer: Dordrecht [astro-ph/0001398]
- van den Heuvel, E. P. J. 1992, in X-ray Binaries and Recycled Pulsars, ed. E. P. J. van den Heuvel and S. A. Rappaport, p.233 (vdH92)
- Webbink, R. F. 1992, in X-ray Binaries and Recycled Pulsars, ed. E. P. J. van den Heuvel and S. A. Rappaport, p.269
- Webbink, R. F., Rappaport, S., & Savonije, G. J. 1983, ApJ, 270, 678

Table 1: Star Formation Rate (SFR) Profiles^a

Model	z_{max}	p	Comments
Peak-M	0.39	4.6	Madau profile
Hierarchical	0.73	4.8	Hierarchical clustering model ^b
Anvil-10	1.49	3.8	Monolithic models
Peak-G	0.63	3.9	“Peak” part of composite Gaussian
Gaussian	N/A	N/A	Gaussian starburst ^c added at high- z

^aModel parameters taken from B99a,b.

^bWe have chosen the B99b model with a dust temperature 45 K. Note that the parameter p for the SFR equals 3/2 plus the value of the parameter p occurring in equation (16) for the merger efficiency in B99b.

^cParameters of Gaussian starburst component (see eq.[6] of text), are from the modified model given in B99b, *i.e.*, $z_p = 1.7$, $\sigma = 1.0$ Gyr, and $\Theta = 70$.

Table 2: Evolution of X-ray Luminosity L_X

Model	τ_{PSNB}	τ_{LMXB}	$\frac{L_X(0.5)}{L_X(0.0)}$	$\frac{L_X(1.0)}{L_X(0.0)}$
Peak-M	1.9	0.1	3.9	5.4
Peak-M	0.9	0.5	4.6	6.8
Peak-M	1.9	1.0	3.4	4.1
Hierarchical	1.9	1.0	6.2	11.3
Anvil-10	1.9	1.0	5.4	10.1
Gaussian	1.9	1.0	7.5	16.0

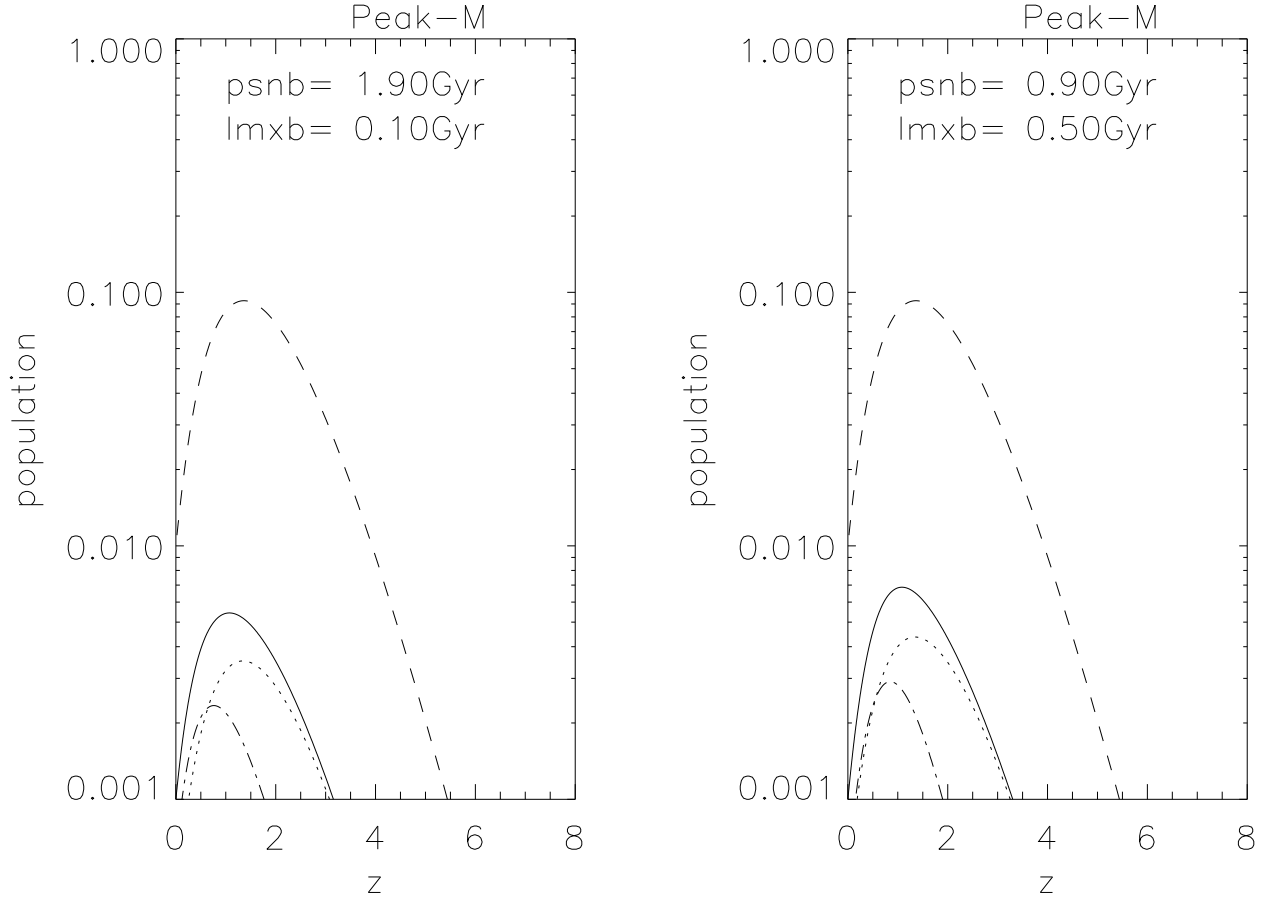


Fig. 1.— Evolution of HMXB population (dotted line), LMXB population (dash-dotted line), and the total X-ray luminosity L_X (solid line) of a galaxy with a given SFR (dashed line). As absolute ordinate scales are irrelevant for these evolutionary profiles, they have been adjusted for convenience of display: L_X always starts at 0.001 at $z = 0$, so that its evolution can be immediately read off the figure, and SFR always starts at 0.01 at $z = 0$, so that different SFR profiles can be readily compared. This figure is for the Peak-M profile (see text), showing the effect of varying the evolutionary timescales τ_{PSNB} and τ_{LMXB} , whose values are written on each panel. The timescales used here are those used in WG98, corresponding to whole LMXB populations and short-period systems.

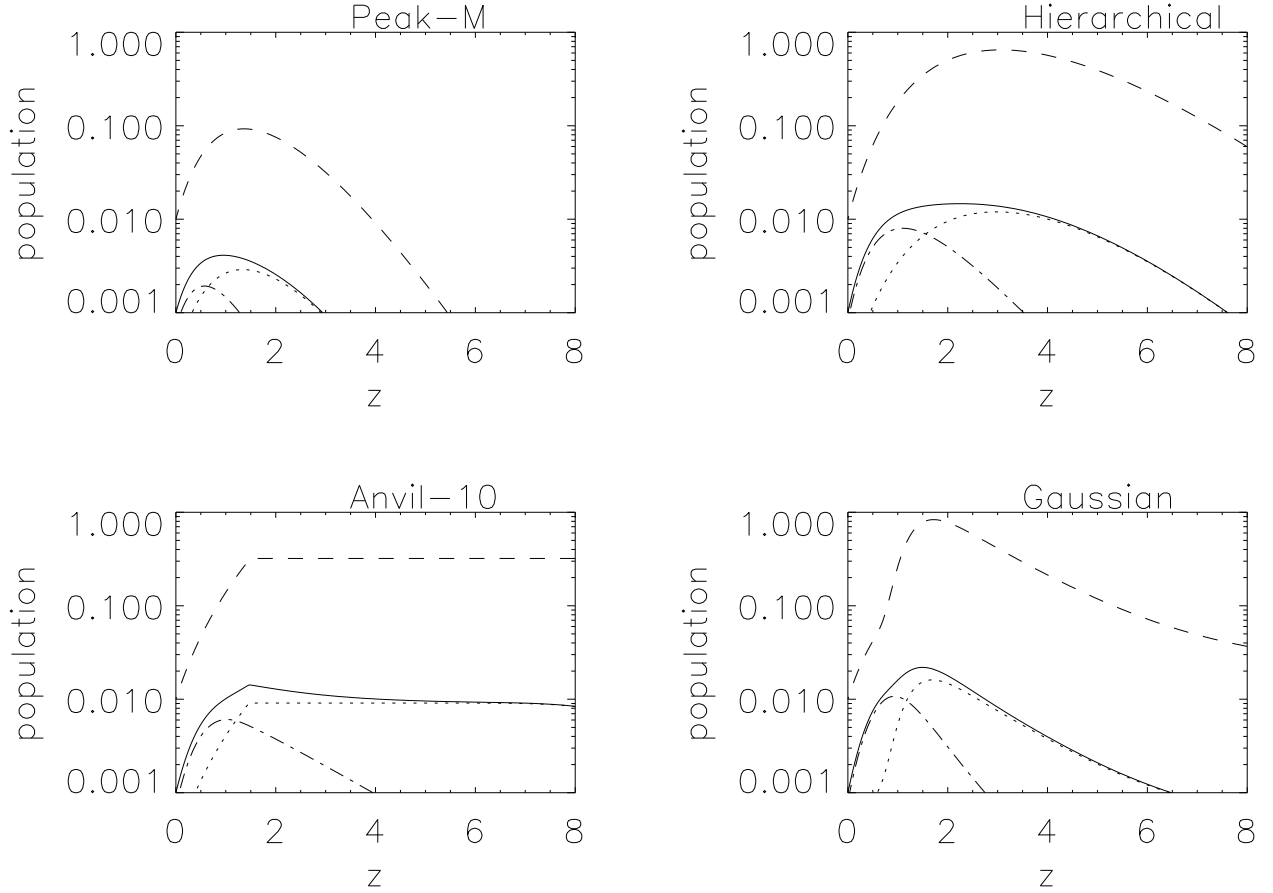


Fig. 2.— Same as Figure 1, but showing the effect of varying the SFR profile. The evolutionary timescales are kept fixed at $\tau_{\text{PSNB}} = 1.9$ Gyr and $\tau_{\text{LMB}} = 1.0$ Gyr for all cases, and SFR profiles from Table 1 are used. Each panel is labeled by the name of its SFR profile. Evolutionary factors from this and the previous figure are collected in Table 2 and described in the text.